arXiv:1411.1886v1 [hep-ex] 7 Nov 2014

SUSY searches at CMS

Alessandro Gaz, *University of Colorado*

On the behalf of the CMS Collaboration.

To appear in the proceedings of the Interplay between Particle and Astroparticle Physics workshop, 18 – 22 August, 2014, held at Queen Mary University of London, UK.

1 Introduction

The recent discovery of the Higgs boson [1] constitutes a magnificent triumph for Particle Physics, but the existence of such elusive particle also poses difficult challenges for the field. The mass of the Higgs boson, not protected by any symmetry, receives quantum corrections from physics at higher scales; these corrections, unless some miraculous fine tuning of the parameters is in place, are expected to raise the mass of the Higgs Boson to a value orders of magnitude higher than the ~ 126 GeV that we have observed.

One of the most popular theories that have been proposed to solve this *Hierarchy Problem* is that of Supersymmetry (SUSY), which postulates the existence, for each particle of the Standard Model (SM), of a *supersymmetric partner* with spin that differs by 1/2 unity from that of the SM particle. The existence of these fermion-boson pairs provides a cancellation mechanism for the corrections of the Higgs mass that greatly reduces the need for a fine tuning of the parameters. In a *natural* scenario, one in which there is only minimal need for fine tuning, the masses of the partners of the $t-$ and $b-$quarks, of the gluon, and of the Higgs bosons are expected to be relatively low, not much above the 1 TeV threshold (see e.g. [2]).

The search for a light $\tilde{t}$ has been one of the keynotes of the early SUSY searches at the LHC, which focused on $\tilde{t}$ pair production with $\tilde{t} \to t\tilde{\chi}_1^0$ as dominant decay channel. These analyses (see e.g. [3]) already provide tight constraints for the Natural SUSY paradigm, but have little sensitivity in particular regions of the phase space in which light $\tilde{t}$ pairs could still be allowed. One such example is the region in which $m_{\tilde{t}} - m_{\chi} \sim m_t$; for this case the stop pair production would not be experimentally distinguishable from the SM $t\bar{t}$ events. Dedicated analyses to cover for these *blind regions* of the classic $\tilde{t}$ searches have thus been developed and some will be presented here.

In $R-$parity conserving scenarios, the Lightest Supersymmetric Particle (LSP) is stable and neutral and thus it constitutes a viable candidate for the Dark Matter in the Universe. In this contributions we focus on these $R-$parity conserving scenarios: the stable (and neutral) LSP does not interact with the detector, thus producing sizable *missing transverse energy* ($E_{\mathrm{T}}^{\mathrm{miss}}$). The results of the different searches are interpreted both using full realistic models (pMSSM, cMSSM, mSugra, ...) and Simplified Models, in which only few specific production and decay processes for the SUSY particles are considered. Most of the attention in the last two years has shifted towards the interpretation of SUSY results in terms of Simplified Models.

2 The CMS Detector at the LHC

The CMS detector is described in detail elsewhere [4]. Charged tracks are measured using silicon pixel and strips detectors, the energies of charged and neutral particles are measured by a lead tungstate electromagnetic calorimeter and by a brass-scintillator hadronic calorimeter. All these detectors are hosted inside a superconducting solenoid, providing a magnetic field of 3.8 Tesla. The flux return yoke is instrumented with gas detectors, that are mainly used for the detection and momentum measurement of muons. The CMS detector has operated reliably during the first years of operations. The results presented here are based on the full 8 TeV $p-p$ dataset delivered by the CERN LHC in 2012. The sample corresponds to an integrated luminosity of ~ 19.5 fb^{-1}.

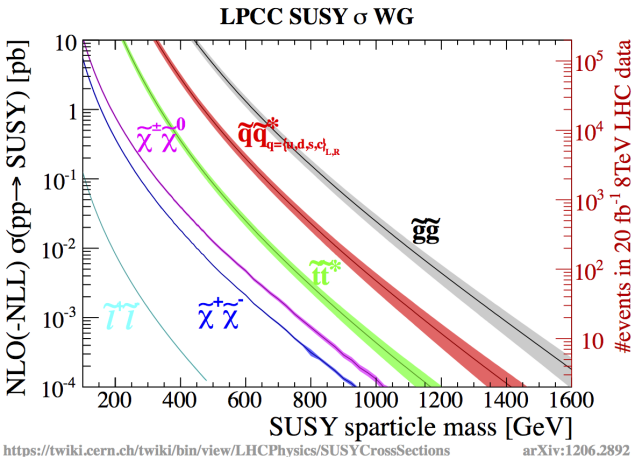

Figure 1: Cross sections for the main SUSY production mechanisms at the LHC, at a $p-p$ collision energy of 8 TeV.

Fig. 1 shows the cross-sections at the LHC for the main production mechanisms of pairs of supersymmetric particles. The production of strongly interacting particles can be already probed at masses above 1 TeV. The production of sleptons, charginos, and electroweakinos is disfavored at a hadron collider, nevertheless their decays often lead to very clean signatures, so that masses around 500 GeV could produce a significant signal in the current dataset.

3 Inclusive (hadronic) searches

Inclusive hadronic analyses target the production of gluinos (that subsequently decay to a $q\bar{q}$ pair and the LSP, possibly through an intermediate $q\tilde{q}$ state) and the direct production of squark pairs. Depending on the specific SUSY model under study, signal events will be characterized by different jet multiplicity and different $b-$jet multiplicity; the latter is a powerful tool to discriminate between third-generation SUSY particles (which are expected to decay dominantly to third generation SM particles) and the first two generations. CMS

searches for these signatures using the M_{T2} variable [5], which is defined as:

$$M_{T2}(m_{\tilde{\chi}}) = \min_{\vec{p}_T^{\,\tilde{\chi}(1)}+\vec{p}_T^{\,\tilde{\chi}(2)}=\vec{p}_T^{\,miss}} \left[\max\left(M_T^{(1)}, M_T^{(2)}\right)\right] , \tag{1}$$

where the minimization satisfies the constraint that the total missing momentum is the sum of the missing momentum of the two LSP's present in the event and the transverse mass $M_T^{(i)}$ is defined as:

$$(M_T^{(i)})^2 = (m^{vis(i)})^2 + m_{\tilde{\chi}}^2 + 2(E_T^{vis(i)} E_T^{\tilde{\chi}(i)} - \vec{p}_T^{\,vis(i)} \vec{p}_T^{\,\tilde{\chi}(i)}) . \tag{2}$$

The M_{T2} variable is designed to be robust against jet energy mismeasurements that could produce fake $E_{\mathrm{T}}^{\mathrm{miss}}$ in hadronic multijet events. The dataset is subdivided into several disjoint signal regions, characterized by different (b-)jet multiplicities and different values of the scalar sum of the transverse momenta of the jets in the event (H_T). The observed event yields are consistent with the background predictions that are derived from several data control samples, so exclusion limits are set, using the signal regions that are expected to be the most sensitive for each model considered. Some exclusion plots are presented in Fig. 2 (left and center).

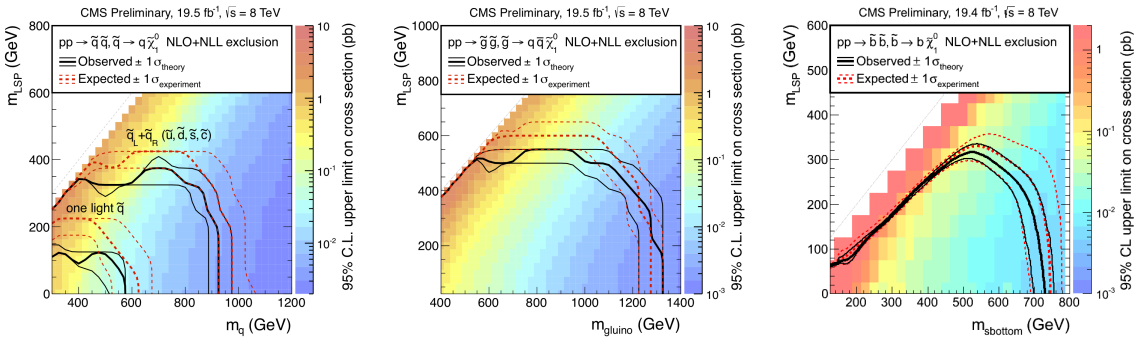
CMS Preliminary, 19.5 fb-1, √s = 8 TeV
pp → q̃q̃, q̃ → qχ̃10 NLO+NLL exclusion
Observed ± 1σtheory
Expected ± 1σexperiment
q̃L+q̃R (ū, d̄, s̄, c̄)
one light q̃
mLSP (GeV)
mq (GeV)
95% C.L. upper limit on cross section (pb)
CMS Preliminary, 19.5 fb-1, √s = 8 TeV
pp → g̃g̃, g̃ → qq̄χ̃10 NLO+NLL exclusion
Observed ± 1σtheory
Expected ± 1σexperiment
mLSP (GeV)
mgluino (GeV)
95% C.L. upper limit on cross section (pb)
CMS Preliminary, 19.4 fb-1, √s = 8 TeV
pp → b̃b̃, b̃ → bχ̃10 NLO+NLL exclusion
Observed ± 1σtheory
Expected ± 1σexperiment
mLSP (GeV)
msbottom (GeV)
95% CL upper limit on cross section (pb)

Figure 2: Exclusion limits for the CMS M_{T2} analysis [5] for direct $\tilde{q}$ pair production (left plot) and gluino production with each gluino decaying to a light $q\overline{q}$ pair and the LSP (center plot). Right plot: exclusion limits for the direct production of $\tilde{b}$ pairs in [6].

Another CMS search [6] targets the direct production of $\tilde{b}$ pairs, selecting events with exactly two jets with $p_T > 70$ GeV, at least one of which is identified as a b-jet. The discriminating variable is M_{CT}, which is defined as:

$$M_{CT}^2(J_1, J_2) = [E_T(J_1) + E_T(J_2)]^2 - [\mathbf{p_T}(J_1) - \mathbf{p_T}(J_2)]^2 \tag{3}$$

$$= 2p_T(J_1)p_T(J_2)(1 + \cos\Delta\phi(J_1, J_2)) . \tag{4}$$

The dominant sources of background for this topology are Z and W + jets events, with $Z \to \nu\nu$ and $W \to \ell\nu$; a single μ data control sample is utilized to predict their contributions

in the signal region. No significant excess over the predicted background is observed, so upper limits on the $\tilde{b}$-pair production are set (see Fig. 2, right).

The monojet search [7] targets the direct $\tilde{t}$-pair production. As mentioned before, there is a strong belief that the mass of the lightest $\tilde{t}$ is relatively low in the SUSY spectrum. Initial $\tilde{t}$ searches focused on the $t\bar{t} + E_{\mathrm{T}}^{\mathrm{miss}}$ signature, excluding direct $\tilde{t}$ pair production up to $m_{\tilde{t}} \sim 700$ GeV for a light LSP (see e.g. [8] for a combination of a single lepton and a razor inclusive CMS analyses). In the case $10 < m_{\tilde{t}} - m_{\chi} < 80$ GeV, the dominant decay is expected to be $\tilde{t} \to c\tilde{\chi}_1^0$. The signature would consist of a soft hadronic jet associated to a limited amount of $E_{\mathrm{T}}^{\mathrm{miss}}$, that would not offer a handle for an efficient separation from the SM backgrounds, unless it recoils against a hard Initial State Radiation (ISR) jet. CMS searches for this signature, selecting events with a hard ISR jet (and allowing for at most one more soft jet). The modeling of the ISR is crucial for this analysis and for other analyses targeting compressed spectra: discrepancies between the data and the simulation are corrected for by using high statistics SM control samples ($t\bar{t}$, Z+jets, ...). Exclusion limits are presented on the left plot of Fig. 3; the sensitivity of the analysis is higher at low values of $m_{\tilde{t}} - m_{\chi}$, where the events appear to be more monojet-like.

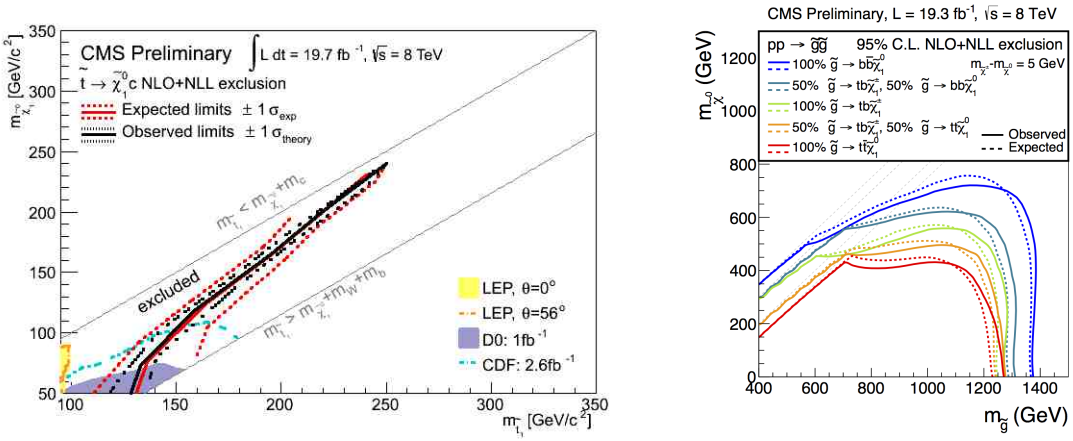
CMS Preliminary
L dt = 19.7 fb -1, √s = 8 TeV
t̃ → χ̃10 c NLO+NLL exclusion
Expected limits ± 1 σexp
Observed limits ± 1 σtheory
excluded
LEP, θ=0°
LEP, θ=56°
D0: 1fb -1
CDF: 2.6fb -1
CMS Preliminary, L = 19.3 fb-1, √s = 8 TeV
pp → g̃g̃ 95% C.L. NLO+NLL exclusion
100% g̃ → bb̄χ̃10
50% g̃ → bb̄χ̃10, 50% g̃ → tt̄χ̃10
100% g̃ → tt̄χ̃10
Observed
Expected

Figure 3: Left: exclusion limits for the monojet search [7]. Right: exclusion limits for gluino pairs production, with gluinos decaying to different mixtures of $b\bar{b}\tilde{\chi}_1^0$, $b\bar{t}\tilde{\chi}_1^0$, and $t\bar{t}\tilde{\chi}_1^0$, obtained by the razor inclusive analysis [8].

Finally, more exclusion limits on gluino pair production have been obtained by the razor inclusive analysis [8]. The branching ratios of the gluino decays are varied from the most favorable final state $b\bar{b}\tilde{\chi}_1^0$ to the most challenging $t\bar{t}\tilde{\chi}_1^0$, see Fig. 3 (right). The difference between the exclusion limits of the two extreme cases (100-150 GeV for low $\tilde{\chi}_1^0$ masses) gives some feeling about the dependence of the results on the assumptions on which simplified models are relying.

4 Kinematic edge in Opposite Sign Dileptons

Electroweakino decay chains, such as $\tilde{\chi}_0^2 \to \tilde{\ell}\ell \to \ell^+\ell^-\tilde{\chi}_1^0$, can produce final states containing opposite-charge same-flavor leptons. The kinematics of this kind of decays is such that the distribution of the invariant mass of the lepton pair has a *triangular* shape, with a sharp endpoint that is defined by the masses (and the mass differences) of the particles involved. CMS performed a search for this kind of signal in its 2012 dataset, selecting opposite sign electron and muon pairs [9], and $E_{\mathrm{T}}^{\mathrm{miss}} > 100$ GeV. Events in which both leptons are *central* ($|\eta| < 1.4$) are considered separately from those containing at least a *forward* lepton ($1.6 < |\eta| < 2.4$). Two strategies are employed for the search:

1. a kinematic fit, using a signal shape defined by the convolution of a triangular shape with a Gaussian:

$$\mathcal{P}(m_{\ell\ell}) = \frac{1}{\sqrt{2\pi}\sigma_{\ell\ell}} \int_0^{m_{\ell\ell}^{edge}} y \cdot \exp\left(-\frac{(m_{\ell\ell}-y)^2}{2\sigma_{\ell\ell}^2}\right) dy\,. \tag{5}$$

   The central and forward regions are fitted simultaneously, with the edge position $m_{\ell\ell}^{edge}$ being constrained to be the same in the two regions.

2. a cut-and-count analysis is performed in the range $20 < m_{\ell\ell} < 70$ GeV, independently for central and forward events.

The backgrounds can be divided in two main categories: *flavor symmetric* (that produce same- or opposite flavor dileptonic events with equal probability) and Drell-Yan (DY), in which only same-flavor pairs are created. The flavor symmetric background (dominated by $t\bar{t}$ events) is studied from $e\mu$ events, and its normalization is corrected for the small reconstruction efficiency differences with respect to the same flavor events. The DY component is estimated using two (independent) methods: the Jet-Z balance method (that relies on the imbalance between the p_T of the Z/γ^* candidate and that of the hadronic system to separate between SM events and a potential signal) and the $E_{\mathrm{T}}^{\mathrm{miss}}$ template method, in which background enriched data control samples are used to extrapolate the contribution at high $E_{\mathrm{T}}^{\mathrm{miss}}$.

Fig. 4 shows the results of the two analysis strategies. Both approaches find a small signal-like excess, with a significance of 2.4 standard deviations for the kinematical fit and 2.6σ (0.3σ) for the cut-and-count analysis in the central (forward) region. While the excess observed is perfectly compatible with a statistical fluctuation of the backgrounds, this is certainly one of the most interesting hints that will deserve further scrutiny at the beginning of the LHC Run2.

5 Searches with photons in the final state

CMS searches for a variety of SUSY models which produce events with at least two photons performing a *razor* analysis [10]. The razor variables for a dijet event are defined as:

$$M_R \equiv \sqrt{(p_{j1}+p_{j2})^2 - (p_z^{j1}+p_z^{j2})^2}\,, \quad R \equiv M_T^R/M_R\,, \tag{6}$$

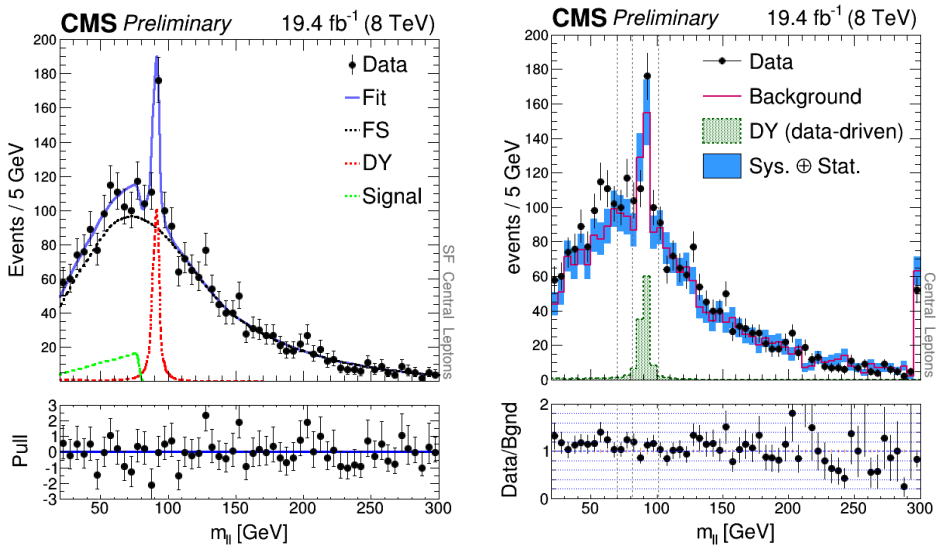

Figure 4: Results of the opposite-sign same-flavor dilepton analysis [9]. Left: fit of the central events; the black dotted line represents the flavor symmetric background (dominated by $t\bar{t}$), the red component is the Drell-Yan background, and the green dotted line corresponds to the small signal-like excess that is seen. Right: results of the cut-and-count analysis for the central events.

where

$$M_T^R \equiv \sqrt{\frac{E_{\mathrm{T}}^{\mathrm{miss}}(p_T^{j1}+p_T^{j2}) - \vec{E}_T^{miss}\cdot(\vec{p}_T^{\,j1}+\vec{p}_T^{\,j2})}{2}}\,. \tag{7}$$

For an event containing multiple objects (jets, photons, leptons), the objects are combined into two *megajets*: the combination which minimizes the quadratic sum of the invariant masses of the two megajets is chosen. Events with at least two isolated photons ($p_T > 30$ and 22 GeV) and at least one hadronic jet with $p_T > 40$ GeV are selected. The data sample is split into a *signal* and a *control* region, defined by the cuts:

- signal: $M_R > 600$ GeV, $R^2 > 0.002$;
- control: $M_R > 600$ GeV, $0.001 < R^2 < 0.002$.

For the models under study, the background contamination is negligibly small in the control region, which is used to fit for the background shape:

$$P(M_R) \propto e^{-k(M_R - M_R^0)^{1/n}}\,, \tag{8}$$

where k, M_R^0, and n are fit parameters. The results are used to derive a prediction for the background in the signal region. No significant excesses are found with respect to the expectations, so limits on a number of SUSY models are set (see Fig. 5).

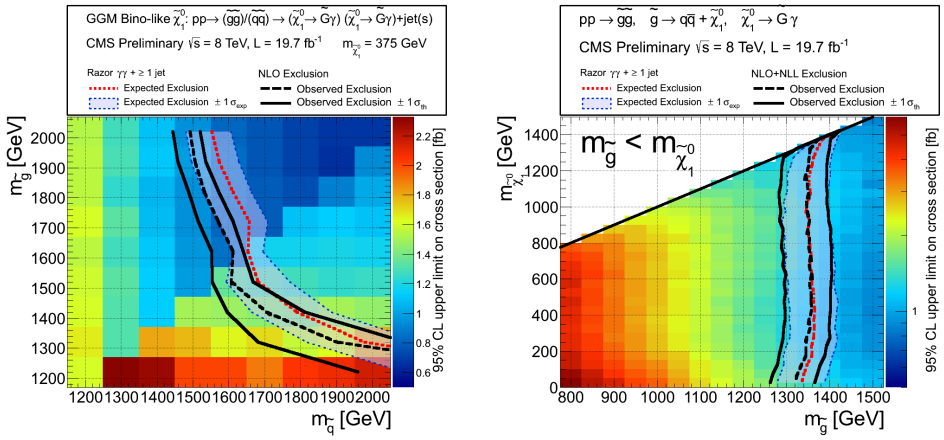
GGM Bino-like $\tilde{\chi}_1^0$: pp→ ($\tilde{g}\tilde{g}$)/($\tilde{q}\tilde{q}$) → ($\tilde{\chi}_1^0$→ Gγ) ($\tilde{\chi}_1^0$→ Gγ)+jet(s)
CMS Preliminary √s = 8 TeV, L = 19.7 fb-1
m$_{\tilde{\chi}_1^0}$ = 375 GeV
Razor γγ + ≥ 1 jet
NLO Exclusion
Expected Exclusion
Expected Exclusion ± 1σexp
Observed Exclusion
Observed Exclusion ± 1σth
m$_{\tilde{g}}$ [GeV]
m$_{\tilde{q}}$ [GeV]
95% CL upper limit on cross section [fb]
pp → $\tilde{g}\tilde{g}$, $\tilde{g}$ → q$\bar{q}$ + $\tilde{\chi}_1^0$, $\tilde{\chi}_1^0$ → G γ
CMS Preliminary √s = 8 TeV, L = 19.7 fb-1
Razor γγ + ≥ 1 jet
NLO+NLL Exclusion
Expected Exclusion
Expected Exclusion ± 1σexp
Observed Exclusion
Observed Exclusion ± 1σth
m$_{\tilde{g}}$ < m$_{\tilde{\chi}_1^0}$
m$_{\tilde{\chi}_1^0}$ [GeV]
m$_{\tilde{g}}$ [GeV]
95% CL upper limit on cross section [fb]

Figure 5: Exclusion limits of the razor photon analysis [10]. Left plot: exclusion in the $m_{\tilde{g}}$ vs $m_{\tilde{q}}$ plane in a General Gauge Mediated scenario, right plot: exclusions for the simplified model in which gluino pairs are produced and each gluino decays to $q\bar{q}\tilde{\chi}_1^0$, with the virtual $\tilde{\chi}_1^0$ decaying to a gravitino $\tilde{G}$ and a photon.

6 Searches with Higgs bosons in the final state

In many SUSY models, Higgs bosons are produced in the final state, both from the decay of strongly interacting sparticles and from electroweakino decays (see Fig. 6).

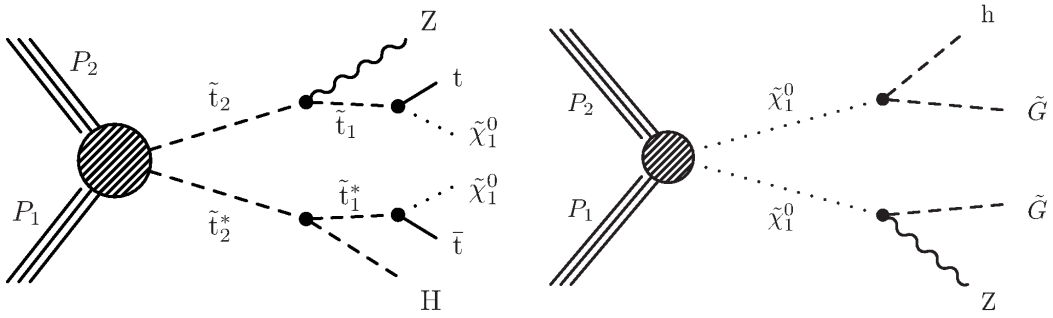

Figure 6: Examples of SUSY scenarios producing at least one SM Higgs boson in the final state. Left: $\tilde{t}_2$ pair production, with $\tilde{t}_2 \to H/Z\,\tilde{t}_1$ investigated in [11]; right: higgsino pair production with $\chi \to H/Z\,\tilde{G}$ searched for by [12].

The first kind of scenarios is investigated by CMS to search for $\tilde{t}_2$ production [11], to target the regions in which the $\tilde{t}_1$ has a mass unfavorable for the classic direct searches. The target model for this analysis includes $\tilde{t}_2$ pair production, with $\tilde{t}_2 \to H/Z\tilde{t}_1$, $\tilde{t}_1 \to t\tilde{\chi}_1^0$. The branching fraction of $\tilde{t}_2$ to H or Z are varied between the two extreme scenarios (100% decays to Higgs bosons or 100% decays to Z's). Three search strategies are employed for

this analysis, selecting the following topologies:

1. events with one lepton or two opposite-sign leptons and at least three b-jets;
2. events with two same-sign leptons and at least one b-jet;
3. events with at least three leptons and at least one b-jet.

The dominant SM backgrounds come from $t\bar{t}$ events and diboson (VV) production; these are suppressed by requiring at least one extra lepton or b-jet with respect to the standard topologies, and with additional requirements on other topological variables like $E_{\mathrm{T}}^{\mathrm{miss}}$, $M_T(\ell, E_{\mathrm{T}}^{\mathrm{miss}})$, ... The observed number of events are consistent with the SM predictions, so limits on the $\tilde{t}_2$ production are set, see Fig. 7. In all cases most of the sensitivity comes from the multilepton channel.

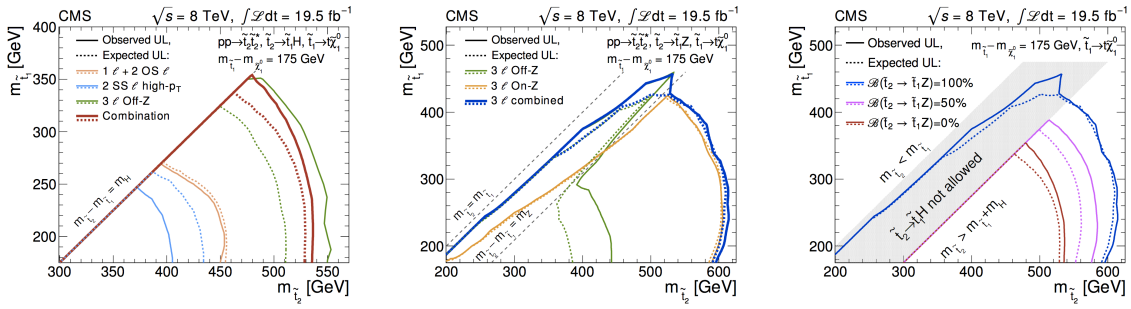

Figure 7: Exclusion limits of [11] for the $\tilde{t}_2 \to H/Z\tilde{t}_1$ simplified model. Left: $\tilde{t}_2 \to H\tilde{t}_1$ (100%), center: $\tilde{t}_2 \to Z\tilde{t}_1$ (100%), right: summary plot with the two extreme cases and the case $\mathrm{BR}(\tilde{t}_2 \to H\tilde{t}_1) = \mathrm{BR}(\tilde{t}_2 \to Z\tilde{t}_1) = 50\%$.

The production of electroweakino pairs and their decays to final states containing Higgs bosons (or Z's and W's) is considered in [12]. In the target scenario, higgsino ($\tilde{\chi}_1^0$) pairs, or $\tilde{\chi}_2^0\tilde{\chi}^{\pm}$ pairs are produced, with $\tilde{\chi}_1^0 \to h\tilde{G}$, ($\tilde{G}$ is an effectively massless gravitino), $\tilde{\chi}_1^0 \to Z\tilde{G}$, $\tilde{\chi}_2^0 \to h\tilde{\chi}_1^0$, and $\tilde{\chi}^{\pm} \to W^{\pm}\tilde{\chi}_1^0$. Several different channels, each with different sensitivity depending on the $\tilde{\chi}_1^0$ mass and on the branching fractions, and associated to a significant amount of $E_{\mathrm{T}}^{\mathrm{miss}}$, are considered:

- For the hh final state: $bb\,bb$, $\gamma\gamma\,bb$, $\gamma\gamma\,WW/ZZ/\tau\tau$;
- For hZ: $\gamma\gamma\,jj$, $\gamma\gamma\,ee/\mu\mu/\tau\tau$, $bb\,ee/\mu\mu$;
- For ZZ: $\geq 3\ell$, $\ell^+\ell^-\,jj$;
- For hW: $\gamma\gamma\,jj$, $\gamma\gamma\,\ell\nu$.

No significant excesses over the SM background expectations are found, so the channels expected to have significant sensitivity to the model under study are combined in a likelihood fit. For the higgsino production scenario, with $\tilde{\chi}_1^0 \to h/Z\tilde{G}$, the limits are evaluated in the

$\mathrm{BR}(\tilde{\chi}_1^0 \to h\tilde{G}) = 1 - \mathrm{BR}(\tilde{\chi}_1^0 \to Z\tilde{G})$ vs $m(\tilde{\chi}_1^0)$ plane, see Fig. 8. For the $\mathrm{BR}(\tilde{\chi}_1^0 \to h\tilde{G}) = 100\%$ case, no exclusion is achieved, even though the multilepton and $bb\,bb$ analyses get limits within 1σ of exclusion at low and intermediate $\tilde{\chi}_1^0$ masses respectively. In the $\mathrm{BR}(\tilde{\chi}_1^0 \to Z\tilde{G}) = 100\%$ case instead, higgsino pair production is excluded up to $m(\tilde{\chi}_1^0) \simeq 380$ GeV.

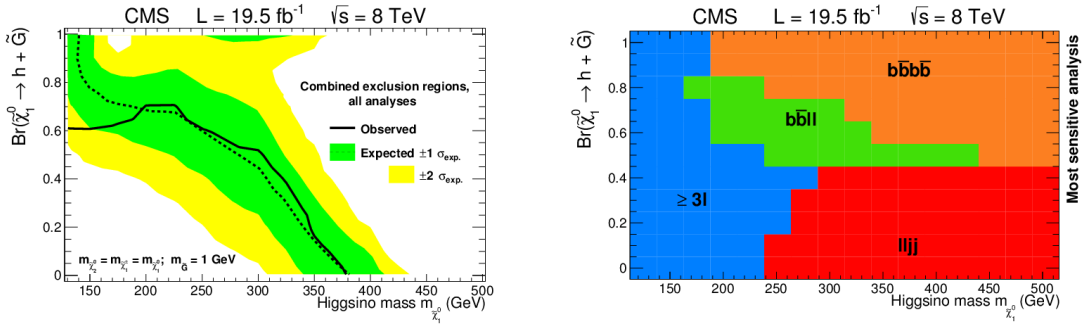
CMS L = 19.5 fb-1 √s = 8 TeV
Br(χ̃10 → h + G̃)
Combined exclusion regions, all analyses
Observed
Expected ±1 σexp.
±2 σexp.
mg̃ = mχ̃2 = mχ̃1; mG̃ = 1 GeV
Higgsino mass mχ̃10 (GeV)
CMS L = 19.5 fb-1 √s = 8 TeV
Br(χ̃10 → h + G̃)
bb̄bb̄
bb̄ll
≥ 3l
lljj
Most sensitive analysis
Higgsino mass mχ̃10 (GeV)

Figure 8: Exclusion limits of [12] on higgsino production. Left plot: limits as a function of the higgsino mass (x axis) and $\mathrm{BR}(\tilde{\chi}_1^0 \to h\tilde{G}) = 1 - \mathrm{BR}(\tilde{\chi}_1^0 \to Z\tilde{G})$ (y axis); the bottom left corner below the black solid line is excluded by the analysis. The right plot shows the most sensitive channel on the same plane contributing to the exclusion.

7 Summary

The CMS Collaboration performed an extensive program of search for the evidence of decays of supersymmetric particles, exploiting the full $p-p$ Run1 dataset, collected at center of mass energies of 7 and 8 TeV. A variety of search strategies has been employed, ranging from inclusive searches, sensitive to a wide spectrum of SUSY topologies, to searches targeting very specific final states. No significant excess has been observed over the Standard Model backgrounds, so stringent limits are set on potential New Physics scenarios.

Despite the lack of discoveries in the Run1 data, the motivation for searching for SUSY signatures at the LHC remains very high as CMS completes the last 8 TeV analyses and prepares for the beginning of the LHC Run2, scheduled for Spring 2015. The increase to a center of mass energy of $13-14$ TeV, along with the large integrated luminosity that will be collected in the next few years, will allow us to significantly extend the sensitivity of SUSY searches and possibly discover or rule out any Natural SUSY scenario.

What has been presented here is a small selection of results and exclusion limits produced by the CMS Collaboration; for more information, please see [13].

8 Acknowledgments

The author would like to thank the IPA 2014 Organizers for the very interesting set of topics, the right balance between talks and discussion, and the relaxed environment in which the Conference took place.

References

[1] G. Aad *et al.* [ATLAS Collaboration], Phys. Lett. B **716**, 1 (2012) [arXiv:1207.7214 [hep-ex]], S. Chatrchyan *et al.* [CMS Collaboration], Phys. Lett. B **716**, 30 (2012) [arXiv:1207.7235 [hep-ex]].

[2] R. Barbieri, D. Pappadopulo, JHEP **0910**, 61 (2009); M. Papucci, J. T. Ruderman, and A. Weiler, JHEP **1209**, 35 (2012).

[3] S. Chatrchyan *et al.* [CMS Collaboration], Eur. Phys. J. C **73**, 2677 (2013) [arXiv:1308.1586 [hep-ex]].

[4] S. Chatrchyan *et al.* [CMS Collaboration], JINST **3** S08004 (2008).

[5] CMS Collaboration, CMS-PAS-SUS-13-019.

[6] CMS Collaboration, CMS-PAS-SUS-13-018.

[7] CMS Collaboration, CMS-PAS-SUS-13-009.

[8] CMS Collaboration, CMS-PAS-SUS-14-011.

[9] CMS Collaboration, CMS-PAS-SUS-12-019.

[10] CMS Collaboration, CMS-PAS-SUS-14-008.

[11] V. Khachatryan *et al.* [CMS Collaboration], Phys. Lett. B **736**, 371 (2014) [arXiv:1405.3886 [hep-ex]].

[12] V. Khachatryan *et al.* [CMS Collaboration], arXiv:1409.3168 [hep-ex], submitted to Phys. Rev. D.

[13] CMS Collaboration, https://twiki.cern.ch/twiki/bin/view/CMSPublic/PhysicsResultsSUS.